SLAC-PEP-NOTE--279

DE89 006219

A SUMMARY OF SOME BEAM-BEAM MODELS

A. W. Chao

Abstract

Two categories of theoretical models for the beam-beam interaction are reviewed: the linear-lens models and the single-resonance models. In a linear-lens model, the beam-beam force is linearized and represented by a localized linear lens. Analyses of incoherent single particle effects can be performed exactly in these models by using matrix techniques. Although the results do not agree with the experimental observations in many respects, the linear-lens models constitute a starting point of our understanding of the beam-beam interaction. In the single-resonance models, one is concerned with the possible incoherent instabilities as the betatron tune of some of the particles is close to a certain rational number. It is assumed in these models that one and only one such rational number dominates the single-particle beam-beam effects. It is found that static single resonances cannot explain many of the experimental results. Some attempts have been made to modify the static single-resonance theory by including some mechanisms for diffusive tune fluctuations or periodic tune modulations. These modified single-resonance models have met only with some limited qualitative success.

Table of Contents

1. Introduction

The subject of the beam-beam interaction has been studied ever since the colliding beam devices were first considered.[1-4] Today, with many colliding beam storage rings in operation, this subject is not yet fully understood. This is evidenced by the fact that many of the existing storage rings have not reached the beam-beam limited design luminosities. The main difficulty is, in fact, a familiar one, i.e., to solve a system with a "nonintegrable" Hamiltonian. Similar difficulty has appeared, o. eventually will appear, in other branches of physics.

Fig. 1 shows the number of papers (that I found in the SLAC library) the storage ring physicists have written on the subject of the beam-beam interaction versus the calendar years. One notices a peak around 1973-1974 and a drop after 1975. This might explain why we urgently need to have a symposium on the subject of beam-beam interaction, since writing review articles (like this one) prevents the curve in Fig. 1 from dropping to zero, at least for 1978-79.

The references considered in Fig. 1 contain experimental studies, numerical simulations, theoretical models and review articles. The theoretical models can roughly be divided into three catagories: the linear-lens models, the single-resonance models and the multiple-resonance models. In the following, we will review some of the linear-lens and the single-resonance models. Other topics are covered by other speakers of this symposium. For simplicity of discussion, we will mainly concern ourselves with collisions of bunched beams.

2. Linear-Lens Models

When two bunched beams collide head-on, a particle in one beam passes through the electromagnetic fields produced by particles in the other beam and receives a transverse impulse. This transverse impulse can be decomposed into a horizontal x-component and a vertical y-component to yield two kicking angles $\Delta x'$ and $\Delta y'$. If the bunch length is short compared with the horizontal and vertical betatron wavelengths at the interaction point, the transverse particle distribution in the x-y plane does not change appreciably during the interaction and the impulse can be considered to be a localized delta function perturbation. For a given transverse particle distribution, the kicking angles $\Delta x'$ and $\Delta y'$ depend on the horizontal displacement x and the vertical displacement y of the particle as it passes through the interaction region. For an upright bi-Gaussian distribution with beam dimensions σ_x and σ_y, for example, we have[5]

$$\Delta x' = -\frac{\partial U(x,y)}{\partial x} \quad \text{and} \quad \Delta y' = -\frac{\partial U(x,y)}{\partial y} , \tag{1}$$

where U(x,y) is the electromagnetic potential well found to be

$$U(x,y) = -\frac{Nr_0}{\gamma}\int_0^{\infty} dt \, \frac{\exp\left[-\frac{x^2}{2(\sigma_x{}^2+t)} - \frac{y^2}{2(\sigma_y{}^2+t)}\right] - 1}{\sqrt{(\sigma_x{}^2+t)\ (\sigma_y{}^2+t)}} \tag{2}$$

with $r_0 = e^2/mc^2$ the classical radius of the particle, N the number of particles in the on-coming particle bunch and γ the relativistic Lorentz factor. In deriving Eq.(1), we have made the approximation that x and y do not change appreciably during the interaction. It is clear from Eq. (1) that the beam-beam force can be written as the gradient of an electromagnetic potential. The source of this potential is a continuum of charge distribution with total charge Ne rather than a collection of N point charges. Effects which are not results of the direct Coulomb interaction (such as the beam-beam Bremstrahlung effect) and effects which are consequences of the interaction between individual particles (such as the Coulomb interaction of two individual particles) are thus excluded from our treatment.

In a linear-lens approximation, we are concerned with particles with small betatron amplitudes so that $x \ll \sigma_x$ and $y \ll \sigma_y$. For those particles, Eq.(1) gives

$$\Delta x' = \pm \frac{2N\, r_0}{\gamma\sigma_x(\sigma_x+\sigma_y)}\, x$$

$$\Delta y' = \pm \frac{2N\, r_0}{\gamma\sigma_y(\sigma_x+\sigma_y)}\, y\,, \qquad (3)$$

where the - signs are used if the electric charges of the two beams have opposite signs and the + signs are used otherwise. In the following we will assume - signs. As seen from Eq.(3), the motion becomes linear and decoupled. In the linear-lens model, it is therefore possible to consider only one degree of freedom, which we choose to be the vertical dimension.

2.1 Incoherent Betatron Effects

The motion of small amplitude particles is conveniently analyzed by using matrix techniques. The transformation matrix for the vector

$$\begin{bmatrix} y \\ y' \end{bmatrix}$$

across the interaction region is, from Eq.(3),

$$\begin{bmatrix} 1 & 0 \\ -1/f & 1 \end{bmatrix} \quad , \quad \frac{1}{f} = \frac{2N\, r_0}{\gamma\sigma_y(\sigma_x+\sigma_y)} \qquad (4)$$

which, we recognize, is the same as the transfer matrix of a thin-lens quadrupole magnet with focal length f. If we let there be one interaction region per superperiod of the storage ring, ν be the unperturbed betatron tune per superperiod and β_0^* be the unperturbed beta-function at the interaction point, the transformation from the middle of one interaction region to the middle of a neighboring interaction region can be written as[6]

$$\begin{bmatrix} \cos 2\pi\,(\nu+\Delta\nu) & \beta^* \sin 2\pi\,(\nu+\Delta\nu) \\ -\frac{1}{\beta^*}\sin 2\pi\,(\nu+\Delta\nu) & \cos 2\pi\,(\nu+\Delta\nu) \end{bmatrix}$$

$$= \begin{bmatrix} 1 & 0 \\ -\frac{1}{2f} & 1 \end{bmatrix} \begin{bmatrix} \cos 2\pi\nu & \beta_0^* \sin 2\pi\nu \\ -\frac{1}{\beta_0^*}\sin 2\pi\nu & \cos 2\pi\nu \end{bmatrix} \begin{bmatrix} 1 & 0 \\ -\frac{1}{2f} & 1 \end{bmatrix} \quad (5)$$

where $\Delta\nu$ is the tune shift caused by the beam-beam perturbation, β^* is the perturbed beta-function at the middle of the interaction region. In the thin-lens model, the transverse beam size scales with the square root of the perturbed beta-function. Solving Eq.(5) yields

$$\cos 2\pi\,(\nu+\Delta\nu) = \cos 2\pi\nu - \frac{\beta_0{}^*}{2f}\sin 2\pi\nu$$
$$\beta^*/\beta_0{}^* = \sin 2\pi\nu/\sin 2\pi\,(\nu+\Delta\nu). \quad (6)$$

It has been hoped, and seriously studied experimentally and theoretically, that one or two dimensionless scaling parameters may describe the beam-beam interaction completely or almost completely. In the linear-lens model, it is clear from Eq.(6) that two such parameters are the unperturbed betatron tune ν and a beam-beam strength parameter defined as[1-4]

$$\xi = \frac{\beta_0{}^*}{4\pi f} \quad (7)$$

A negative sign must be added to Eq.(7), yielding $\xi < 0$, if the electric charges of the two beams are of the same sign. The factor 4π is included so that, when ξ is small, the beam-beam tune shift $\Delta\nu$ is equal to ξ. Note that it is the unperturbed β_0^* that goes into the definition of ξ. The factor β_0^* can be thought of as a magnification factor which, when applied to a perturbation, gives the effectiveness of the perturbation on the particle's betatron motion. To reduce the effect of the beam-beam interaction, it is advantageous to reduce the value of β_0^*. This leads to the idea of low-β^* insertion that has been successfully used to increase the luminosity of many storage rings.

Using the two parameters ν and ξ as coordinates, we have plotted in Figs. 2 and 3 countours of constant $\Delta\nu$ and β^*/β_0^*. The value of ν is restricted in 0 and 1/2 since it is periodic with period 1/2. The shaded area indicates a region with no stable solution. The width, $\delta\nu$, of this unstable region for a given ξ is given by

$$\delta\nu = \frac{1}{\pi} \tan^{-1} 2\pi\xi \tag{8}$$

for small ξ, $\delta\nu \approx 2\xi$.

For a given storage ring configuration, one would like to know, at least qualitatively, the behavior of luminosity $\mathscr{L}$ as a function of the number of particles N in each beam. To do this, one first notices that as N is changed, the values of ξ and β^* change according to Eq.(6) and the expression $\xi \propto N/\beta^*$ in a self-consistent manner, and that it is this self-consistent solution of β^* that must be substituted in the expression $\mathscr{L} \propto N/\beta^*$ to find the dependence of $\mathscr{L}$ on the number of particles N. This is done using a computer and the results are illustrated in Fig. 4 on a full logarithmic graph paper. The units are arbitrary. The dotted line represents the value of $\mathscr{L}$ without taking into account the changes in β^*. For large ν (i.e., close to 1/2), $\mathscr{L}$ is consistently below the dotted line, while for small ν, $\mathscr{L}$ can be above the dotted line; but in both cases, $\mathscr{L}$ tends to level off as N is increased indefinitely. To optimize the luminosity, this result suggests that the betatron tune per superperiod be slightly above (below if $\xi < 0$) a half-integer or integer.

Many predictions of the linear-lens model do not agree with the experimental observations. For example, we seem to observe that the beam-beam perturbation does couple the x- and y-motions; the transverse beam sizes do not seem to scale with the square root of the perturbed beta-functions; and the beam-beam instability seems to appear with a beam intensity well below the stability limit indicated in Figs. 2 and 3. On the other hand, the linear-lens model does describe physically the motion of small amplitude particles. It also has the advantage of being easy to analyze and can serve as a starting point of further adventures.

2.2 Incoherent Synchrotron Effects

Although the linearized beam-beam perturbation does not couple the x- and y-motions as is indicated by Eq.(3), it can still couple the x- or y-motion to the longitudinal synchrotron degree of freedom under some conditions.[7-8] In this section, we will show this by an example, using the linear-lens approximation and matrix techniques.

Consider two beams, one strong and one weak, crossing each other vertically at an angle 2α. We can look for the betatron and synchrotron tune shifts as well as changes in particle distribution of the weak beam under the influence of the collisions with the strong beam. To do this, we consider a particle in the weak beam with no horizontal displacement, and with vertical displacement y and longitudinal displacement z relative to the beam center. The impulse that this particle receives from each crossing is given by, in the relativistic limit,

$$\frac{\Delta\vec{p}}{p_0} = -\frac{G\,\hat{n}}{\cos\alpha}\int_0^{y\cos\alpha - z\sin\alpha} dt\,\exp\left(-\frac{t^2}{2\Sigma^2}\right) \tag{9}$$

which, after linearization, becomes[7]

$$\frac{\Delta\vec{p}}{p_0} = -G\,\hat{n}\,(y - z\tan\alpha) \tag{10}$$

where

$$G = \frac{2 N r_0}{\gamma \sigma_x \Sigma}$$

$$\Sigma^2 = \sigma_z^2 \sin^2 \alpha + \sigma_y^2 \cos^2 \alpha$$

and $\hat{n}$ is the unit vector shown in Fig. 5; σ_x, σ_y and σ_z are the rms beam width, beam height and bunch length of the strong beam. This impulse, which contains a vertical component and a longitudinal component, provides a coupling mechanism between the y- and z-motions. The longitudinal component of $\Delta\vec{p}$ causes the energy of the particle to change by an amount

$$\Delta\delta = \frac{\Delta p_z}{p_0} = G \sin \alpha \, (y - z \tan \alpha), \qquad (11)$$

$$\delta = \text{relative energy error } \Delta E/E,$$

and the vertical component gives a kick to the particle

$$\Delta y' = \frac{\Delta p_y}{p_0} = - G \cos \alpha \, (y - z \tan \alpha) \, . \qquad (12)$$

If we define a vector

$$\begin{bmatrix} y \\ y' \\ z \\ \delta \end{bmatrix}$$

we obtain from Eqs. (11) and (12) that the transfer matrix of this vector for the beam-beam crossing can be written as

$$T_1 = \begin{bmatrix} 1 & 0 & 0 & 0 \\ -G \cos \alpha & 1 & G \sin \alpha & 0 \\ 0 & 0 & 1 & 0 \\ G \sin \alpha & 0 & -G \tan \alpha \sin \alpha & 1 \end{bmatrix} \qquad (13)$$

The transfer matrix between two neighboring interaction points, assuming no y-z coupling aside from the beam-beam perturbation, is

$$T_2 = \begin{bmatrix} \cos 2\pi\nu_y & \beta_0^* \sin 2\pi\nu_y & 0 & 0 \\ -\frac{1}{\beta_0^*} \sin 2\pi\nu_y & \cos 2\pi\nu_y & 0 & 0 \\ 0 & 0 & a & b \\ 0 & 0 & c & d \end{bmatrix} \tag{14}$$

where $ad-bc = 1$, $a + d = 2 \cos 2\pi\nu_s$ and $b = -\eta L$. The momentum compaction factor η , the total path length L and the tunes $\nu_{y,s}$ refer to the values per superperiod. The total transformation per superperiod is given by $T_0 = T_2 T_1$.

The eigenvalues, λ , of T_0 satisfy

$$\det (T_0 - \lambda) = 0$$

or

$$\left(\frac{\lambda^2+1}{2\lambda} - \cos 2\pi\nu_y + \frac{\beta_0^* G}{2} \sin 2\pi\nu_y\right)\left(\frac{\lambda^2+1}{2\lambda} - \cos 2\pi\nu_s - \frac{\alpha^2}{2} G\eta L\right) = -\frac{1}{4}\alpha^2 \beta_0^* G^2 \eta L \sin 2\pi\nu_y . \tag{15}$$

The four solutions of Eq.(15) for λ are related to the perturbed betatron and synchrotron tunes by $\lambda = \exp(\pm i 2\pi\nu)$. For stability, the perturbed tunes must be real, or equivalently, all four λ's must satisfy $|\lambda| = 1$. It can be shown after some algebra that this stability condition is satisfied outside a stopband around the synchro-betatron resonances $\nu_y \pm \nu_s$ = integer, with a stopband width[8]

$$\delta\nu \approx \begin{cases} \frac{1}{\pi}\left(\frac{\beta_0^* \ G^2 \eta L \alpha^2}{\sin 2\pi\nu_y}\right)^{1/2} & \text{if } \sin 2\pi\nu_y > 0 \\ 0 & \text{if } \sin 2\pi\nu_y < 0 \end{cases} \tag{16}$$

If we set $\beta_0^* G = 0.6$, $\alpha = 1$ mrad, $\nu_y = 0.1$, $\eta L = 2m$ and $\beta_0^* = 0.2m$, the stopband width is found to be 8×10^{-4}.

It is also possible to find from the transfer matrix T_0 the changes in particle distribution. The matrix T_0, which describes the motion of a single particle in the weak beam, has two eigenmodes. The eigenmode axes lie in the y-z plane but are tilted relative to the y-z axes. The weak beam is oriented in such a way that the principle axes of the beam distribution coincide with these eigenmode axes. Knowing T_0, we can thus obtain the tilting angle θ (see Fig. 5) by looking for the eigenmode axes of T_0. The result, assuming $|\alpha| \ll 1$ and $|\beta_0^* G| \ll 1$, is

$$\theta \approx \frac{\beta_0^* G \alpha \sin 2\pi\nu_y}{2(\cos 2\pi\nu_y - \cos 2\pi\nu_s)} \tag{17}$$

To see the effect of this beam tilt on luminosity, we note that in order to avoid any appreciable loss of luminosity, one must have

$$\theta \lesssim \sigma_y/\sigma_z$$

From Eq.(17) we find that this condition is fulfilled if we stay enough distance away from the synchro-betatron resonances, i.e.,

$$|\nu_y \pm \nu_s - K| \geq \delta\nu$$

where K is some integer and $\delta\nu$ is given by

$$\delta\nu = \frac{\sigma_z}{\sigma_y}\frac{\beta_0^* G\alpha}{2\pi} \tag{18}$$

If $\sigma_z/\sigma_y = 600$, $\beta_0^* G = 0.6$ and α = 1mrad, we find $\delta\nu$ = .06. Comparing this value with the stopband width found following Eq. (16), we find that the luminosity may suffer from the beam-beam synchro-betatron coupling even well outside of the unstable stopband region.

It should be mentioned that another possible example of beam-beam longitudinal effects is obtained by considering a head-on collision of two beams at a location with finite energy dispersion.[8] The x- and z-motions are coupled in this case. The linear-lens model and the matrix techniques can be used here as well.

Still another synchro-betatron coupling effect caused by the beam-beam perturbation occurs when the bunch length σ_z is not small compared with the beta-function β_0^* at the interaction point. Particles with different longitudinal positions, z, within a bunch arrive at the interaction point at different times, with a time spread of σ_z/c. If σ_z is not small compared with β_0^*, the transverse particle distribution will change appreciably in the time duration of σ_z/c. The transverse beam-beam kick received by a particle then depends on the longitudinal position of the particle, causing a synchro-betatron coupling effect. This effect, whose leading term is quadratic in z, cannot be treated by the linear-lens model.

2.3 Coherent Effects

So far we have been considering the incoherent motion of a single particle under the influence of the beam-beam collisions. It turns out that the beam-beam interaction can also excite coherent bunch oscillations, in which each bunch behaves like a rigid distribution of particles, while the center-of-mass of the bunches oscillate.[9] In the linear-lens approximation, coherent effects are again analyzed by using matrix methods.

Let us consider a storage ring with two counter-rotating colliding bunches of equal intensity, one bunch in each beam. There are two interaction points and two superperiods. The kicking angles experienced by the two rigid bunches passing through each other are

$$\Delta y_+' = -\frac{1}{f}(y_+ - y_-) = -\Delta y_-' \tag{19}$$

where $y_{+,-}$ are the vertical displacements of the bunch centers relative to the unperturbed trajectory and the focal length f has been defined in Eq.(4). If we describe the coherent motion by the vector

$$\begin{bmatrix} y_+ \\ y_+' \\ y_- \\ y_-' \end{bmatrix},$$

the transfer matrix for the beam-beam collision is

$$T_1 = \begin{bmatrix} 1 & 0 & 0 & 0 \\ -\frac{1}{f} & 1 & \frac{1}{f} & 0 \\ 0 & 0 & 1 & 0 \\ \frac{1}{f} & 0 & -\frac{1}{f} & 1 \end{bmatrix} \tag{20}$$

The total transformation per superperiod is $T_0 = T_2 T_1$, where T_2 is the transfer matrix between two neighboring collision points:

$$T_2 = \begin{bmatrix} \cos 2\pi\nu & \beta_0^* \sin 2\pi\nu & 0 & 0 \\ -\frac{1}{\beta_0^*} \sin 2\pi\nu & \cos 2\pi\nu & 0 & 0 \\ 0 & 0 & \cos 2\pi\nu & \beta_0^* \sin 2\pi\nu \\ 0 & 0 & -\frac{1}{\beta_0^*} \sin 2\pi\nu & \cos 2\pi\nu \end{bmatrix} \tag{21}$$

The eigenvalues of T_0, determined from det $(T_0 - \lambda) = 0$, are found to be two complex conjugate pairs

$$e^{\pm 2\pi i \nu} \quad \text{and} \quad e^{\pm 2\pi i(\nu + \Delta\nu)}$$

with

$$\cos 2\pi(\nu+\Delta\nu) = \cos 2\pi\nu - 4\pi\xi \sin 2\pi\nu \qquad (22)$$

The first pair corresponds to the "0-mode" in which the two bunches move up and down together in phase at the interaction points. The bunches do not feel the beam-beam forces and the mode frequency is equal to the unperturbed betatron frequency. This mode is always stable. The second pair of eigenvalues corresponds to the "π-mode" in which the two bunches move out of phase. The beam-beam force seen by a bunch center with displacement y is the same as that for a single particle with displacement $2y$ in the incoherent motion. Eq.(22) is thus the same as Eq. (6) with $\xi \to 2\xi$. In order for the π-mode to be stable, the absolute value of the right hand side of Eq.(22) must be less than 1. For a given ξ, the value of ξ must be less than a certain stability limit ξ_{limit}. Fig. 6 shows the behavior of ξ_{limit} as a function of ν. It repeats with a period of $\nu = 1/2$. The stability limit for the single particle motion is twice of ξ_{limit}. For a given ξ, the coherent motion is unstable if ν is within a distance $\frac{1}{\pi}\tan^{-1}(4\pi\xi) \approx 4\xi$ below (above if $\xi < 0$) a half-integer or integer.

It should be pointed out that operating colliding beams inside the stopband does not necessarily mean losing the bunch because as soon as the oscillation amplitude grows beyond a sizeable fraction of the beam size, the beam-beam force becomes much weaker than the linear-lens model predicts. However, even a stable π-mode oscillation can be harmful to the luminosity since the beams simply miss each other most of the time.

We now consider another example with six colliding bunches, three bunches in each beam. The storage ring has six interaction points. The analysis of this example follows closely that of the previous example of two bunches; but the vector, shown below in a horizontal row, is now 12-dimensional:

$$[y_{+1}\ \ y'_{+1}\ \ y_{+2}\ \ y'_{+2}\ \ y_{+3}\ \ y'_{+3}\ \ y_{-1}\ \ y'_{-1}\ \ y_{-2}\ \ y'_{-2}\ \ y_{-3}\ \ y'_{-3}]\ .$$

where the first six coordinates refer to the + beam, the other six refer to the - beam. Indices 1, 2, 3 refer to different bunches within one beam. The transfer matrix for bunch +1 to collide with bunch -1 and bunch +2 to collide with bunch -2 and bunch +3 to collide with bunch -3 is a 12 x 12 matrix

$$T_1 = \begin{bmatrix} - & B \\ B & A \end{bmatrix}$$

where

$$A = \begin{bmatrix} 1 & 0 & 0 & 0 & 0 & 0 \\ -\frac{1}{f} & 1 & 0 & 0 & 0 & 0 \\ 0 & 0 & 1 & 0 & 0 & 0 \\ 0 & 0 & -\frac{1}{f} & 1 & 0 & 0 \\ 0 & 0 & 0 & 0 & 1 & 0 \\ 0 & 0 & 0 & 0 & -\frac{1}{f} & 1 \end{bmatrix} \qquad B = \begin{bmatrix} 0 & 0 & 0 & 0 & 0 & 0 \\ \frac{1}{f} & 0 & 0 & 0 & 0 & 0 \\ 0 & 0 & 0 & 0 & 0 & 0 \\ 0 & 0 & \frac{1}{f} & 0 & 0 & 0 \\ 0 & 0 & 0 & 0 & 0 & 0 \\ 0 & 0 & 0 & 0 & \frac{1}{f} & 0 \end{bmatrix} \qquad (23)$$

At the next collision, bunches +1, +2 and +3 will collide with bunches -2, -3 and -1, respectively, and the transfer matrix is

$$T_2 = \begin{bmatrix} A & C \\ D & A \end{bmatrix}$$

where

$$C = \begin{bmatrix} 0 & 0 & 0 & 0 & 0 & 0 \\ 0 & 0 & \frac{1}{f} & 0 & 0 & 0 \\ 0 & 0 & 0 & 0 & 0 & 0 \\ 0 & 0 & 0 & 0 & \frac{1}{f} & 0 \\ 0 & 0 & 0 & 0 & 0 & 0 \\ \frac{1}{f} & 0 & 0 & 0 & 0 & 0 \end{bmatrix} \qquad D = \begin{bmatrix} 0 & 0 & 0 & 0 & 0 & 0 \\ 0 & 0 & 0 & 0 & \frac{1}{f} & 0 \\ 0 & 0 & 0 & 0 & 0 & 0 \\ \frac{1}{f} & 0 & 0 & 0 & 0 & 0 \\ 0 & 0 & 0 & 0 & 0 & 0 \\ 0 & 0 & \frac{1}{f} & 0 & 0 & 0 \end{bmatrix} \tag{24}$$

The next collision is +1, +2 and +3 against -3, -1 and -2, with the transfer matrix

$$T_3 = \begin{bmatrix} A & D \\ C & A \end{bmatrix} \tag{25}$$

In between collisions, the transfer matrix is

$$R = \begin{bmatrix} r & 0 & 0 & 0 & 0 & 0 \\ 0 & r & 0 & 0 & 0 & 0 \\ 0 & 0 & r & 0 & 0 & 0 \\ 0 & 0 & 0 & r & 0 & 0 \\ 0 & 0 & 0 & 0 & r & 0 \\ 0 & 0 & 0 & 0 & 0 & r \end{bmatrix} \qquad r = \begin{bmatrix} \cos 2\pi\nu & \beta_o^* \sin 2\pi\nu \\ -\frac{1}{\beta_o} \sin 2\pi\nu & \cos 2\pi\nu \end{bmatrix} \tag{26}$$

where $2\pi\nu$ is the betatron phase advance between two neighboring interaction points. The total transformation for one superperiod (3 collisions, half a revolution) is

$$T_0 = RT_3 \, RT_2 \, RT_1 \tag{27}$$

The six eigenmodes of T_0 describe the six coherent beam-beam modes. The coherent motion is stable if and only if all eigenvalues of T_0 have absolute values of unity. In Fig. 7, the stability limit of the beam-beam parameter, ξ_{limit}, is plotted vs. ν (which is 1/6 of the unperturbed betatron tune). For a given $\xi \ll 1$, the coherent motion is unstable if ξ is within a distance 4ξ below (above if $\xi < 0$) 1/2, or within a distance 2ξ below 1/3, or within a distance 2ξ below 1/6. In a range of ν of 1/2, this amounts to a total stopband width of 8ξ. It is clear that the unstable region occupys most of the available ν-space if ξ is something like 0.06.

3. Single-Resonance Models

In a linear-lens model, the highly nonlinear beam-beam force is linearized. The particle motion can be analyzed exactly by using matrix methods. We found that the single particle motion is completely described by two parameters: the betatron tune per superperiod ν and the strength parameter ξ. We also found that if ν is sufficiently close to n/2 with n an integer, the particle motion becomes unstable.

It turns out[10-15] that the particle motion is affected by the beam-beam perturbation when ν is close to a rational number n/p, and the linear-lens model has only treated the case for p = 2. Unfortunately, it is not possible to perform an exact analysis for $p \neq 2$, since nonlinear terms in the beam-beam force must be included. To proceed, we make two drastic assumptions:

- there is one and only one rational number n/p which dominates the single particle motion; and (28)
- the "smooth approximation" (see later) holds.

These assumptions are drastic because, first of all, there must be infinitely more rational numbers which are closer to ν than n/p as long as ν is not exactly equal to n/p. One then argues that only smaller values of p, say $p < 10$, are worth considering because resonances of order higher than $\sim$10 do not affect the particle motion too much. This will be partially justified later. Secondly, the "smoothing" procedure has excluded some physical phenomena from being studied, one example of which is the existence of "stochastic layers" in the phase space.[16]

In the following, we will insist on the assumptions (28). A static single-resonance model, for which parameters such as ν and ξ are static in time, is first discussed. The method of analysis is well-defined in this model and will be included in some detail. Unfortunately, according to this model, the particle motion is always stable against the beam-beam perturbation, in disagreement with the experimentally observed decrease of beam lifetime when beams collide.

To explain this discrepancy, we seem to have two alternatives. One alternative is to keep the two assumptions (28) but modify the static model to include time-dependent parameters. This alternative is discussed in Section 3.2, but only very briefly for the reason that the conclusions of some of these models seem more convincing than the analyses which lead to these conclusions. Another alternative is to relax the assumptions (28) by considering multiple resonances or by numerical studies of the stochastic layers. This alternative will not be discussed here since it is better covered by other speakers of this symposium.

3.1 The Static Model

The motion of a particle under the influence of the beam-beam perturbation is described by the Hamiltonian

$$H = \frac{1}{2}(p_x^2 + K_x x^2) + \frac{1}{2}(p_y^2 + K_y y^2) + U(x,y)\,\delta(s)\ , \qquad (29)$$

where U(x,y) is defined in Eq.(2), and the aximuthal coordinate s had been defined so that the beam-beam collision occurs at s = 0. The equations of motion are

$$\frac{d^2 z}{d^2 s} + K_z(s) z = -\frac{\partial U}{\partial z}\,\delta(s) \;, \quad z = x, y \;. \tag{30}$$

Before we apply the single-resonance approximation, we need to make three successive canonical transformations on this Hamiltonian: a Courant-Snyder transformation,[6] an action-angle transformation and a slow-variable transformation.[10] It is not necessary to carry out each transformation individually. The three transformations can be combined into a single one whose generating function is[17]

$$G(x,y,\psi_x,\psi_y) = -\frac{x^2}{2\beta_x(s)}\left[\tan\phi_x - \frac{\beta_x'(s)}{2}\right] - \frac{y^2}{2\beta_y(s)}\left[\tan\phi_y - \frac{\beta_y'(s)}{2}\right]$$

with (31)

$$\phi_z = \psi_z + \nu_{zo}\frac{s}{R} + \int_0^s ds'\left(\frac{1}{\beta_z(s')} - \frac{\nu_z}{R}\right) \;, \quad z = x, y$$

where $\beta_{x,y}$ are the beta-functions, $2\pi R$ is the circumference of the storage ring, $\phi_{x,y}$ are the betatron phases, ν_{xo} and ν_{yo} are the resonant tune values satisfying $\nu_x \approx \nu_{xo}$, $\nu_y \approx \nu_{yo}$ and $q\nu_{xo} + p\nu_{yo} = n$ (q, p and n are integers). Since $\phi_{x,y} \approx \nu_{x,yo}\frac{s}{R}$, the variables $\psi_{x,y}$ changes slowly in time. The canonical variables before transformation are x, p_x, y, p_y. After transformation the canonical variables are ψ_x, J_x, ψ_y, J_y. The two sets of coordinates are related by

$$z = \sqrt{2J_z\beta_z}\cos\phi_z$$

$$p_z = \sqrt{-\frac{2J_z}{\beta_z}}\left[\sin\phi_z - \frac{\beta_z'}{2}\cos\phi_z\right],\; z = x,y\,. \tag{32}$$

The Hamiltonian after the canonical transformation is

$$K = (\nu_x-\nu_{xo})\,J_x + (\nu_y-\nu_{yo})J_y + K_1$$

with (33)

$$K_1 = \delta(\theta)\,U\left[\sqrt{2J_x\beta_x}\cos(\psi_x+\nu_{xo}\theta),\sqrt{2J_y\beta_y}\cos(\psi_y+\nu_{yo}\theta)\right]$$

We have changed the time variable from s to $\theta = s/R$. The value of $\beta_{x,y}$ in K_1 are taken at the collision point.

So far no approximation has been made. We now make the two assumptions mentioned previously, i.e., (1) we consider one and only one set of integers q, p and n so that $q\nu_x + p\nu_y \simeq n$ and (2) we will separate the beam-beam perturbation Hamiltonian K_1 into a fast oscillating term and a slowly changing term and make the smooth approximation that the fast oscillating term can be ignored.

The perturbation Hamiltonian K_1 can be decomposed into Fourier series:

$$K_1 = \sum_{\alpha,\beta=-\infty}^{\infty} f_{\alpha\beta}(J_x,J_y)\,e^{i\alpha(\psi_x+\nu_{xo}\theta) + i\beta(\psi_y+\nu_{yo}\theta)} \cdot \frac{1}{2\pi}\sum_{\gamma} e^{i\gamma\theta} \tag{34}$$

The slowly changing terms in K_1 are those terms in Eq.(34) whose exponent satisfies $\alpha = kq$, $\beta = kp$ and $\gamma = -kn$. Keeping only those terms in K_1 yields

$$K_1 \approx \frac{1}{2\pi} \sum_{k=-\infty}^{\infty} f_{(kq)(kp)}(J_x, J_y)\; e^{ik(q\psi_x + p\psi_x)} \tag{35}$$

Note that we have included all the slow terms corresponding to the resonant conditions $kq\nu_x + kp\nu_y = kn$ (k = any integer). Substituting the explicit expression of U from Eq.(2) and the Fourier coefficients

$$f_{(kq)(kp)} = \frac{1}{4\pi^2} \int_0^{2\pi} d\theta_x \int_0^{2\pi} d\theta_y \; e^{-ikq\theta_x - ikp\theta_y}$$

$$\times\; U\left(\sqrt{2J_x\beta_x}\cos\theta_x,\; \sqrt{2J_y\beta_y}\cos\theta_y\right)$$

into Eq.(35) and summing over k, one gets

$$K_1 \approx -\frac{1}{4\pi^2}\,\frac{Nr_o}{\gamma}\int_0^{2\pi} d\theta_x \int_0^{2\pi} d\theta_y \sum_{s=-\infty}^{\infty} \delta(q\theta_x + p\theta_y - q\psi_x - p\psi_y + 2\pi s)$$

$$\times \int_0^{\infty} \frac{dt}{\sqrt{(\sigma_x^2 + t)(\sigma_y^2 + t)}} \left\{ \exp\left[-\frac{J_x\beta_x \cos^2\theta_x}{\sigma_x^2 + t} - \frac{J_y\beta_y \cos^2\theta_y}{\sigma_y^2 + t} \right] - 1 \right\} \tag{36}$$

Expression (36) can be written as $\frac{Nr_o}{\gamma}$ times a dimensionless factor which depends on the dimensionless quantities

$$q,\; p,\; q\psi_x + p\psi_y,\; J_x\beta_x/\sigma_x^2,\; J_y\beta_y/\sigma_y^2 \text{ and } \sigma_y/\sigma_x$$

The quantities $q\psi_x + p\psi_y$ and $J_z\beta_z/\sigma_z^2 \equiv \alpha_z$, $z = x,y$ are the dynamical quantities describing the particle's coordinates. The equations of motion, derived from the Hamiltonian K and written in terms of $q\psi_x + p\psi_y$, α_x and α_y, contains these dimensionless parameters:

$$\frac{Nr_0\beta_x}{\gamma\sigma_x^2},\quad \frac{Nr_0\beta_y}{\gamma\sigma_y^2},\quad \frac{\sigma_y}{\sigma_x},\quad p,\ q,\ q\nu_x + p\nu_y - n.$$

The first three are replaceable by

$$\xi_x = \frac{Nr_0\beta_x}{2\pi\gamma\sigma_x(\sigma_x+\sigma_y)},\quad \xi_y = \frac{Nr_0\beta_y}{2\pi\gamma\sigma_y(\sigma_x+\sigma_y)}\cdot\frac{\sigma_y}{\sigma_x}$$

The other three quantities are determined from the values of ν_x and ν_y. We thus conclude that the single-resonance model is completely described by the scaling parameters ξ_x, ξ_y, ν_x, ν_y and σ_y/σ_x.

In the following, we will ignore the x-y coupling by the beam-beam interaction and consider only the vertical motion of a particle. The Hamiltonian of this case is obtained from Eq.(36) by setting $\sigma_x \gg \sigma_y$ and $q = 0$. The resonant terms included in the single-resonance model are

$$\nu \approx \frac{\pm n}{\pm p},\ \frac{\pm 2n}{\pm 2p},\ \frac{\pm 3n}{\pm 3p},\ \text{etc.}$$

The Hamiltonian is

$$K = (\nu - \frac{n}{p})\, J + K_1(J,\psi)$$

$$K_1 = -\frac{\xi}{\beta}\sum_{s=0}^{p-1}\frac{1}{p}\int_0^\infty \frac{dt}{\sqrt{1+t/\sigma_y^2}}\left|\exp\left[-\frac{\alpha\cos^2(\psi-\frac{2\pi s}{p})}{1+t/\sigma_y^2}\right]-1\right| \qquad (37)$$

$$\alpha = J\beta/\sigma_y^2$$

We have dropped some subscripts y. The perturbation Hamiltonian K_1 is independent of n. This is due to the fact that the beam-beam perturbation is a δ-function kick.

It is customary to expand K_1 into Fourier series in ψ. The result is

$$K_1 = -\frac{Nr_0\sigma_y}{\pi\gamma\sigma_y}\left\{1 + \sum_s{}' G_{sp}(\alpha)\cos sp\psi\right\}$$

where (38)

$$G_{sp}(\alpha) = (-1)^{\frac{sp}{2}}\frac{2}{(1+\delta_{s0})(s^2p^2-1)}e^{-\frac{\alpha}{2}}\left[(1+\alpha)I_{\frac{sp}{2}}(\tfrac{\alpha}{2})+\alpha I'_{\frac{sp}{2}}(\tfrac{\alpha}{2})\right]$$

and $\sum_s{}'$ means summing over s from 0 to ∞, but keeping only terms with sp = even, δ_{s0} is the kronecker delta function and $I_{sp/2}$ is the Bessel function. Note that if p is odd, the perturbation Hamiltonian for a resonance of order p is identical to that of order 2p. Note also that sometimes we keep only the first two terms in the Fourier expansion (39). This is based on the approximation that ν is close to $\frac{\pm n}{\pm p}$ but away from $\pm 2n/\pm 2p$, $\pm 3n/\pm 3p$, etc. We decided not to do that since we discovered that $\pm n/\pm p$ is equal to $\pm 2n/\pm 2p$. The reason that only even terms appear in Eq.(38) is due to the fact that we have assumed head-on collision of symmetric bunches.

The equations of motion, obtained from the Hamiltonian K, are

$$\psi' = \nu - \frac{n}{p} - 2\xi\sum_s{}' G'_{sp}(\alpha)\cos sp\psi$$

(39)

$$\alpha' = 2\xi\sum_s{}' sp\, G_{sp}(\alpha)\sin sp\psi.$$

The particle motion is completely described by the two scaling parameters ν (and hence p and $\nu - \frac{n}{p}$) and ξ.

The third term on the right hand side of the ψ' equation gives the effective tune shift of a particle whose slow coordinates are α and ψ. For small amplitude particles with $\alpha \to 0$, it is equal to $\xi\ (1 + \cos 2\psi)$ if p = 1 or 2 and ξ otherwise. The s = 0 term in the $\sum_s{}'$ summation defines a "detuning" contribution:

$$\Delta\nu(\alpha) = -2\xi\, G'_{op}(\alpha) = \xi\, e^{-\frac{\alpha}{2}} \left[I_o(\tfrac{\alpha}{2}) + I'_o(\tfrac{\alpha}{2})\right] \qquad (40)$$

Note that the detuning $\Delta\nu$ is independent of p, the order of the resonance under consideration. A particle with $\alpha = 0$ has a perturbed tune $\nu + \xi$, a particle with $\alpha \to \infty$ has a tune ν and a particle with α between 0 and ∞ has a tune between ν and $\nu + \xi$. The rest of the terms in the summation define a "resonance width" (in tune unit):

$$\delta\nu_p(\alpha) = 4\xi \sum_{s\neq o}{}' |G'_{sp}(\alpha)| \qquad (41)$$

The effective tunes of a group of particles with a given amplitude α and arbitrary phase ψ occupy a spread within $\pm\delta\nu_p/2$ around the detuned value $\nu + \Delta\nu(\alpha)$. The influence of resonances on particle motion is qualitative sketched in Fig. 8. Particles with amplitude α are strongly influenced by resonances if $\nu + \Delta\nu(\alpha)$ lies inside a shaded region.

If the tune is far away from all significant resonances, the above results are still applicable if we keep only the s = 0 term in the summation $\sum_s{}'$. In this special case, the detuning is the same as Eq.(40) but there are no resonance widths. It follows from Eq.(39) that α is a constant of the motion and, since the perturbed tune $\nu + \Delta\nu$ depends only on α, the tune distribution of the beam can be obtained once the distribution in α is known.[11]

In Fig. 9, we have plotted $\delta\nu_p$ versus particle amplitude α for

$\xi = 0.03$ and for several values of p. For odd p, $\delta\nu_p$ is identical to $\delta\nu_{2p}$. For even p, $\delta\alpha_p$ is generally smaller for larger p. This partially justifies the assumptions made in Eq.(28).

Sometimes it is more convenient to define a resonance width $\delta\alpha^{1/2}$ (in unit of $\alpha^{1/2}$) to be the difference between the maximum and the minimum values of $\alpha^{1/2}$ along the separatrix (see Fig 10a below). Let $\alpha_0^{1/2}$ be the average value of $\alpha^{1/2}$ around the separatrix, $\delta\alpha^{1/2}$ is roughly given by

$$\delta\alpha^{1/2} \approx \left(\frac{\sum'_{s\neq 0} |G_{sp}(\alpha_0)|}{2\alpha_0 |G''_{0p}(\alpha_0)|} \right)^{1/2} \tag{42}$$

Note that under this definition, we are no longer interested in the dependence of resonance width on the particle amplitude α. One should not, however, take the definitions of resonance width too seriously since they are not rigorously defined quantities and serve only as order of magnitude concepts. More accurate description of particle motion must be obtained from the equations of motion (39).

The particle trajectories in phase space follow constant Hamiltonian contours. Topologically, there are two types of constant Hamiltonian countours, as illustrated in Figs. 10a and 10b. Particle motion is stable if the contours look like Fig. 10a because the amplitudes are always bounded. The same thing is not true if the contours look like that of Fig. 10b.

For the case of the beam-beam interaction, consider the Hamiltonian K, Eq.(37), at large values of J. As $J \to \infty$, we find that $K_I \propto \sqrt{J}$ is dominated by the $(\nu - \frac{n}{p})J$ term, indicating that the constant Hamiltonian contours at large amplitudes are circles. The Hamiltonian describing the beam-beam interaction, therefore, belongs to the type shown in Fig. 10a, indicating stable single particle motion. Physically, this follows from the fact that a particle crossing the collision point with large amplitude experiences little perturbation from the on-coming beam. One explicit example of beam-beam phase space topology with $p = 6$, $\nu - \frac{n}{p} = -0.01$ and $\xi = 0.06$ is shown in Fig. 11.

3.2 Dynamic Models

In the previous section, we found that a static single-resonance model, in which all beam-beam parameters such as ν and ξ stay constant in time, does not provide an instability mechanism. This somewhat unexpected result disagrees with the experimental observations. In this section, we will briefly discuss the possibility of modifying the static model to include time-varying parameters. It is hoped that such dynamic single-resonance models may explain away the discrepancy.

There seem to be two types of time-dependences that have been studied. In the first type (the trapping model)[18], a beam-beam parameter modulates in time more or less sinusoidally with a certain frequency, while in the second type (the diffusion model)[19-20], a diffusion behavior of the parameter is believed to be the source of the beam-beam instability. Each model suggests a mechanism which continuously brings particles from small betatron amplitudes to larger amplitudes. A physical aperture limitation on the amplitude then explains the observed particle loss in colliding beams. For simplicity of discussion, we will consider the case of electron-positron collisions and assume that the time-varying parameter is the tune ν .

We first consider the trapping model. In the static model, a particle streams along a constant Hamiltonian coutour in the phase space. The topology of these contours depends on the Hamiltonian and, from Eq.(37), depends in turn on the distance from resonance $\nu - \frac{n}{p}$. In the trapping model, the tune of a particle oscillates slowly around or close to the resonant value $\frac{n}{p}$. As a consequence, resonance islands like those shown in Fig. 11 move in and out quasi-statically and, when doing so, distort and relocate phase space area elements. An analysis of the particle motion under these conditions is extremely difficult. As a rough qualitative description, however, we note that a particle is either trapped or not trapped by the resonance islands which are moving from small to large amplitudes. For particles that are trapped, the amplitude grows with the islands. For particles that are not trapped, the amplitude is essentially unperturbed by the passing islands. Particle loss is then a consequence of having the islands trap particles and move them to the physical aperture limit.

To determine the probability that a particle of amplitude α will be trapped by the passing islands, one needs to know the total area A_0 of the islands and the instantaneous growth rate of the amplitude of the islands α_0'. It is suggested that the trapping probability per island passing is proportional to A_0 and decreases more or less exponentially with increasing α_0'.

Fig. 12 sketches the expected behavior of trapping probability P_T as a function of particle amplitude α as the islands sweep through this amplitude with a certain speed. One notices that P_T increases with α for small α and decreases with α for large α. A peak occurs somewhere around $\alpha \sim 1$-3, depending on the order of resonance p under consideration. A typical particle trapping event looks perhaps like this: As the islands move outward in phase space, their trapping efficiency increases and trap a particle at a relatively small amplitude (say, $\alpha \sim 0.5$). The particle then moves outward together with the islands. As the islands move out further, their trapping efficiency starts to decrease and the islands become leaky. The particle will then be dropped from the islands at a larger amplitude (say, $\alpha \sim 5$). We have sketched this process in Fig. 13. The shaded area indicates the region where trapping is efficient. Outside this region, the islands are leaky. The aperture limit can be either inside or outside the shaded region. It is believed in the trapping model that this mechanism may explain the observed decrease of colliding beam lifetime. This trapping mechanism also suggests a possible halo structure in the beam distribution.

The time modulation assumed in the trapping model may come from several sources. For example, the tune may be modulated with the synchrotron frequency f_s in accordance with the particle energy through chromaticity effects; or, if the bunch length is not small compared with the beta-function at the collision point, the parameter ξ may be modulated by the longitudinal position of the particle with the frequency $2f_s$.

A second type of dynamic single-resonance model is the diffusion model. In the presence of the usual radiation damping and quantum diffusion effects of an electron beam,[21] the particle distribution reaches an equilibrium state ρ. Without perturbations, ρ is a gaussian distribution in the particle amplitude. A quantum lifetime of the beam is then determined by the particle diffusion rate of this distribution across the physical aperture limit. It is conceivable that the distortion pf phase space by the presence of a single resonance will also distort the equilibrium distribution, hence reducing the associated quantum lifetime for a given aperture limit. It is clear that one needs to solve for ρ from a Fokker-Planck type of diffusion equation[21], taking simultaneously into account the damping, diffusion and the single resonance contributions. Some attempts have been made in this direction but unfortunately hindered by the very difficult mathematics.[19-20] Nevertheless, as an illustration, let us perhaps write

$$\rho \sim \exp(-gK) \tag{43}$$

where K is the Hamiltonian found in Eq. (37). This expression reduces to the correct gaussian distribution in the limit $\xi \to 0$ if we choose $g = \beta/|\nu - \frac{n}{p}|\, \sigma_0^2$ where β is the beta-function and σ_0 is the natural rms beam size in the absence of beam-beam perturbation. Eq. (43) is approximately valid if the beam-beam perturbation is not too strong so that $p|\nu - \frac{n}{p}| \gg \xi$. It is also correct in the limit of no damping, no diffusion and arbitrary ξ. Under these conditions, we expect the effective physical aperture limit to be reduced by an amount roughly of the order of the resonance width $\delta\alpha^{1/2}$ and the beam lifetime to be shortened accordingly.

Note that the equilibrium particle distribution, Eq. (43), contains a structure of islands just like the Hamiltonian does. Note also that if the tune is away from all resonances, the beam-beam perturbation contributes only a phasewise streaming term in the ψ' equation while keeping $\alpha' = 0$; the beam lifetime will not be affected in that case.

The diffusion mechanism mentioned above does not have to be the quantum diffusion. The momentum diffusion caused by intrabeam scattering for example, can cause a tune diffusion through the chromaticity effect.[19-20]

In addition to those parameters such as $\nu - \frac{n}{p}$, p and ξ, typical for a single-resonance theory, the dynamic models suggest that a few more parameters might be important candidates for determining the beam-beam stability limit: the synchrotron frequency f_s, the chromaticity C and the physical aperture limit A.

References

Out of the 119 references considered in Fig. 1, I have read about 25% and understood about 10%. Most of the references listed below belong to those I happen to have read and not necessarily those I have understood.

1. F.Amman and D.Ritson, "Space-Charge Effects in Electron-Electron and Positron-Electron Colliding or Crossing Beam Rings", Intern. Conf. on High Energy Accel., Brookhaven, 471 (1961).
2. E.D.Courant, "Beam Instabilities in Circular Accelerators", IEEE Trans. on Nucl. Scien., NS-12, 550 (1965).
3. D.Ritson and J.Rees, "Limitations on Storage Ring Reaction Rates", SLAC-TN-65-39 (1965).
4. M.Bassetti, "Numerical Computations of Space Charge Effects in a Positron and Electron Storage Ring",V-th Inter. Conf. on High Energy Accel., Frascati, 708 (1965).
5. B.W.Montague, "Calculation of Luminosity and Beam-Beam Detuning in Coasting Beam Interaction Regions", CERN/ISR-GS/75-36 (1975).
6. E.D.Courant and H.S.Snyder, Ann. of Phys. 3, 1 (1958).
7. L.E.Augustin, "Space Charge Effects in e+e- Storage Ring with Beams Crossing at an Angle", Orsay Note Interne 35-69 (1969).
8. A.Piwinski, "Limitation of the Luminosity by Satellite Resonances", DESY 77/18 (1977).
9. A.Piwinski, "Coherent Beam Break-up due to Space Charge", VIII-th Intern. Conf. on High Energy Accel., Geneva, 357 (1971). A.W. Chao and E. Keil, CERN/ISR note, in preparation (1979).
10. A.Schoch, "Theory of Linear and Nonlinear Perturbations of Betatron Oscillations in Alternating Gradient Synchrotrons", CERN Report 57-23 (1957).

11. A.Jejcic and J.LeDuff, "Non-Linear Beam-Beam Effect", VIII-th Intern. Conf. on High Energy Accel., Geneva 354 (1971).
12. E.Keil, "Nonlinear Space Charge Effects, I", CERN/ISR-TH/72-7 (1972).
13. E.Keil, "Nonlinear Space Charge Effects, II", CERN/ISR-TH/72-25(1972).
14. A.G.Ruggiero and L.Smith, "Calculation of Resonance Effects Due to a Localized Gaussian Charge Distribution". PEP-52 (1973).
15. G.H.Rees, W.T.Toner and J.V.Trotman, "Effects of Beam-Beam Forces in Large Electron-Positron Storage Rings", IEEE Trans. on Nucl. Scien., NS-22, 1447 (1975).
16. L.J.Laslett, IX-th Intern. Conf. on High Energy Accel., Stanford, 394 (1974).
17. L.Smith, private communications (1975).
18. M.Month, "Nature of the Beam-Beam Limit in Storage Rings", IEEE Trans. on Nucl. Scien., Vol. NS-22, 1376 (1975).
19. H.G.Hereward, "Diffusion in the Presence of Resonances", CERN/ISR-DI/72-26 (1972).
20. J.LeDuff, "About the Diffusion Process in the Nonlinear Beam-Beam Effect", CERN/ISR-AS/74-53 (1974).
21. H. Bruck, Accelerateurs Circulaire de Particules (Press Universitaires de France, Paris, 1966)

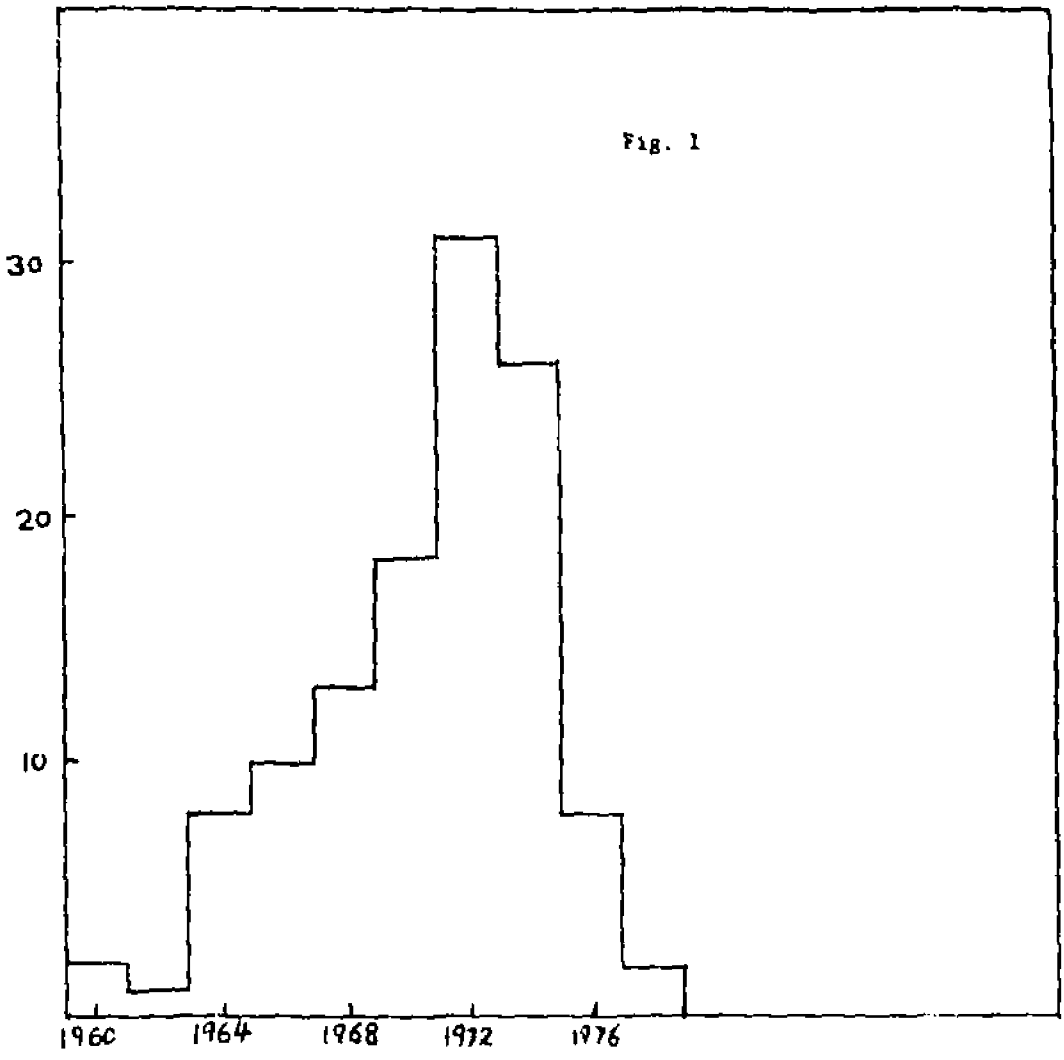
Fig. 1
30
20
10
1960
1964
1968
1972
1976

Fig. 2

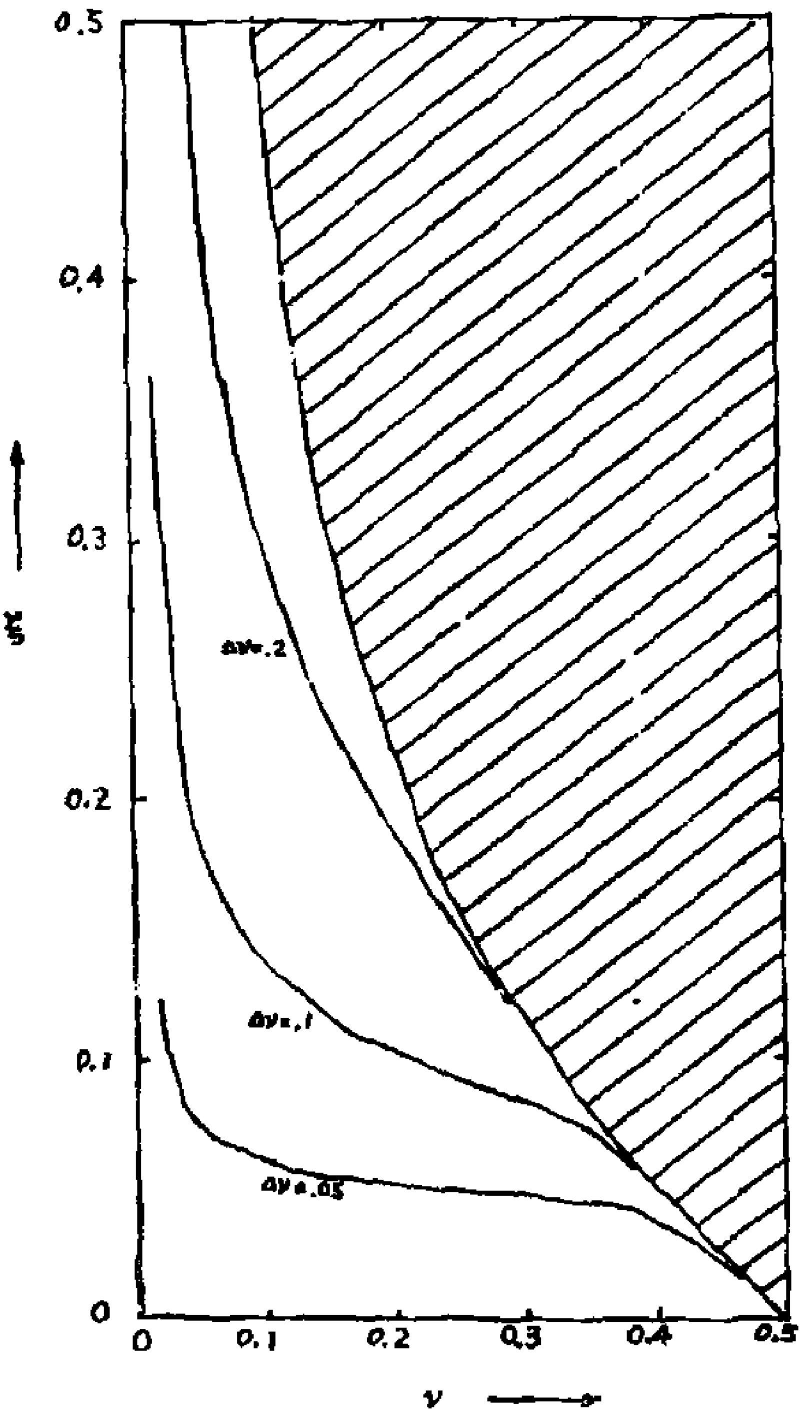

Fig. 3

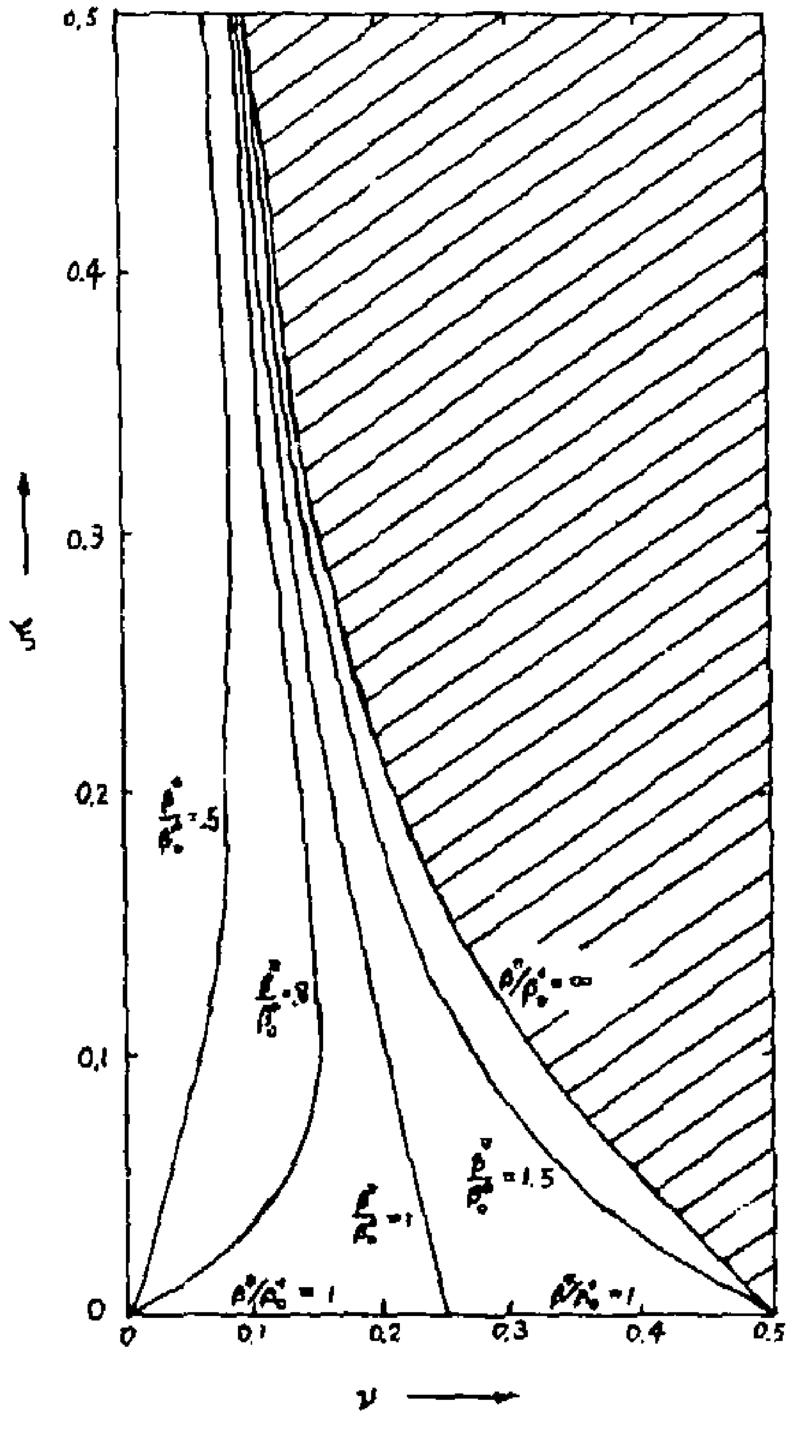
0,5
0.4
0,3
0,2
0,1
0
ξ
0
0,1
0,2
0,3
0,4
0,5
ν
ρ*/ρ*₀ = .5
ρ*/ρ*₀ = .8
ρ*/ρ*₀ = 1
ρ*/ρ*₀ = 1.5
ρ*/ρ*₀ = ∞
ρ*/ρ*₀ = 1
ρ*/ρ*₀ = 1

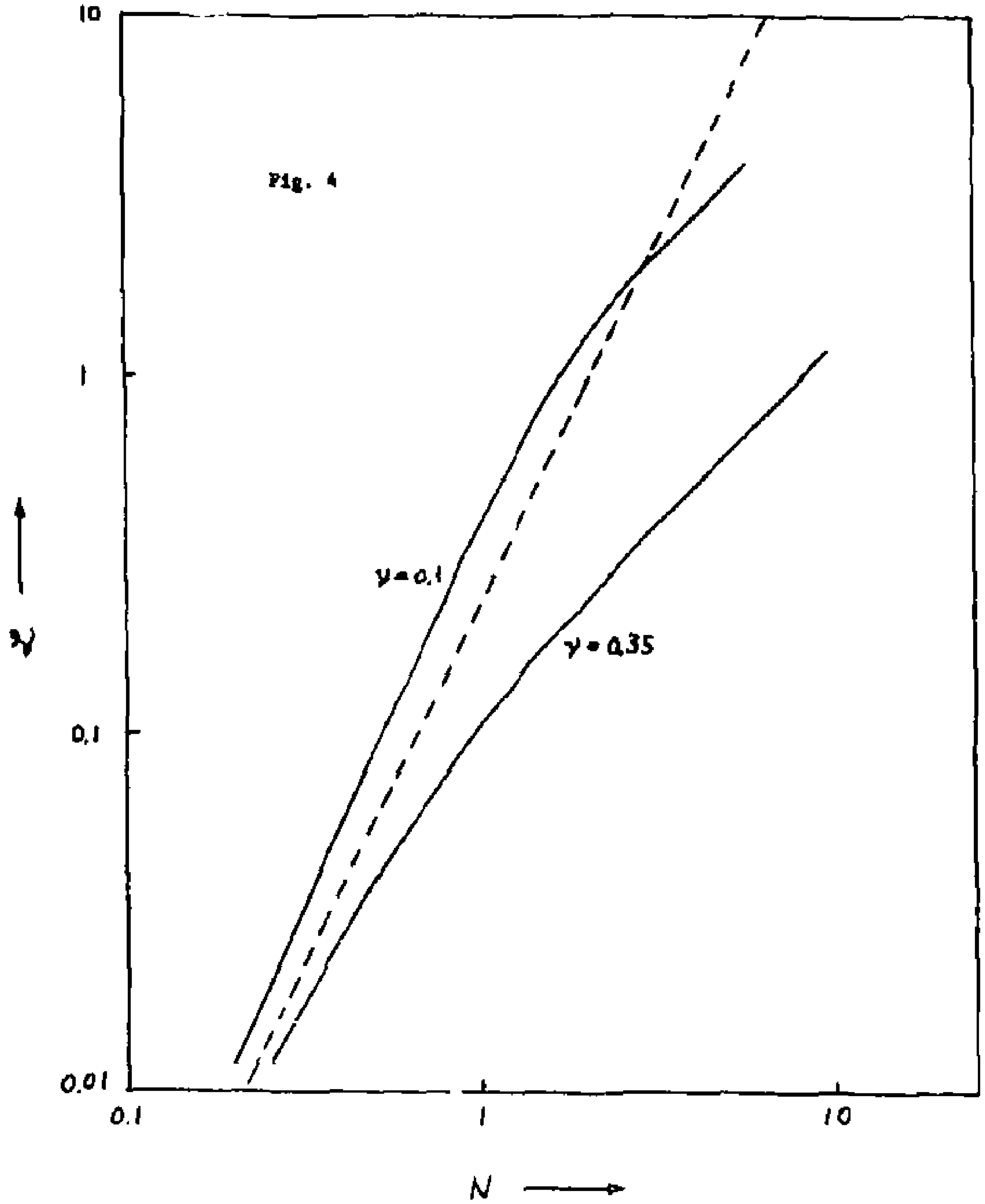

Fig. 4

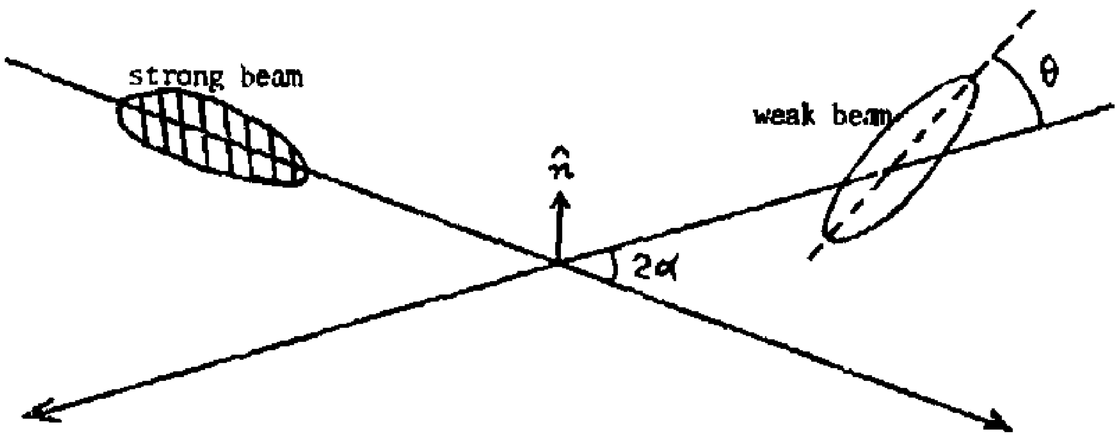

Fig. 5

Fig. 6

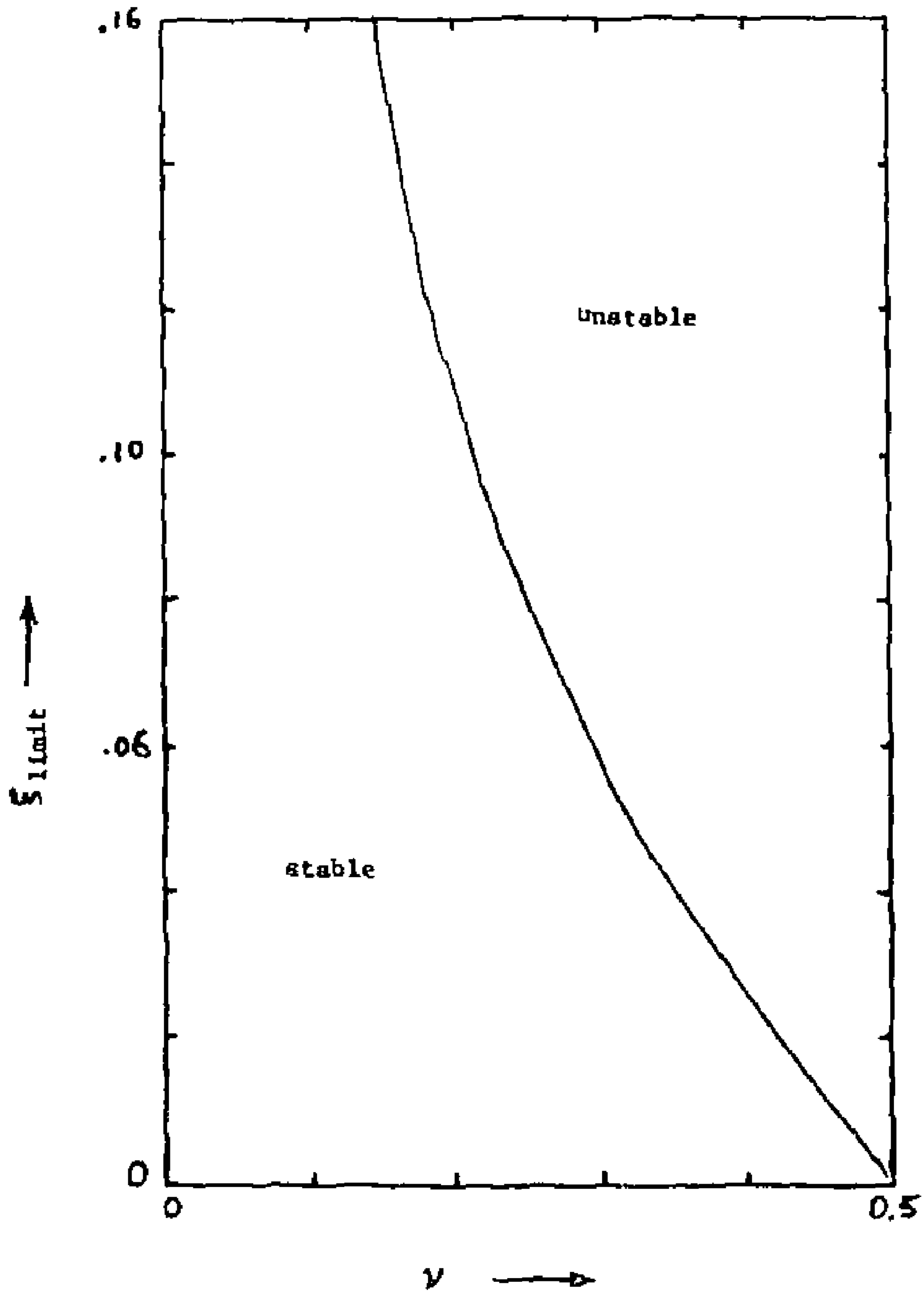

Fig. 7

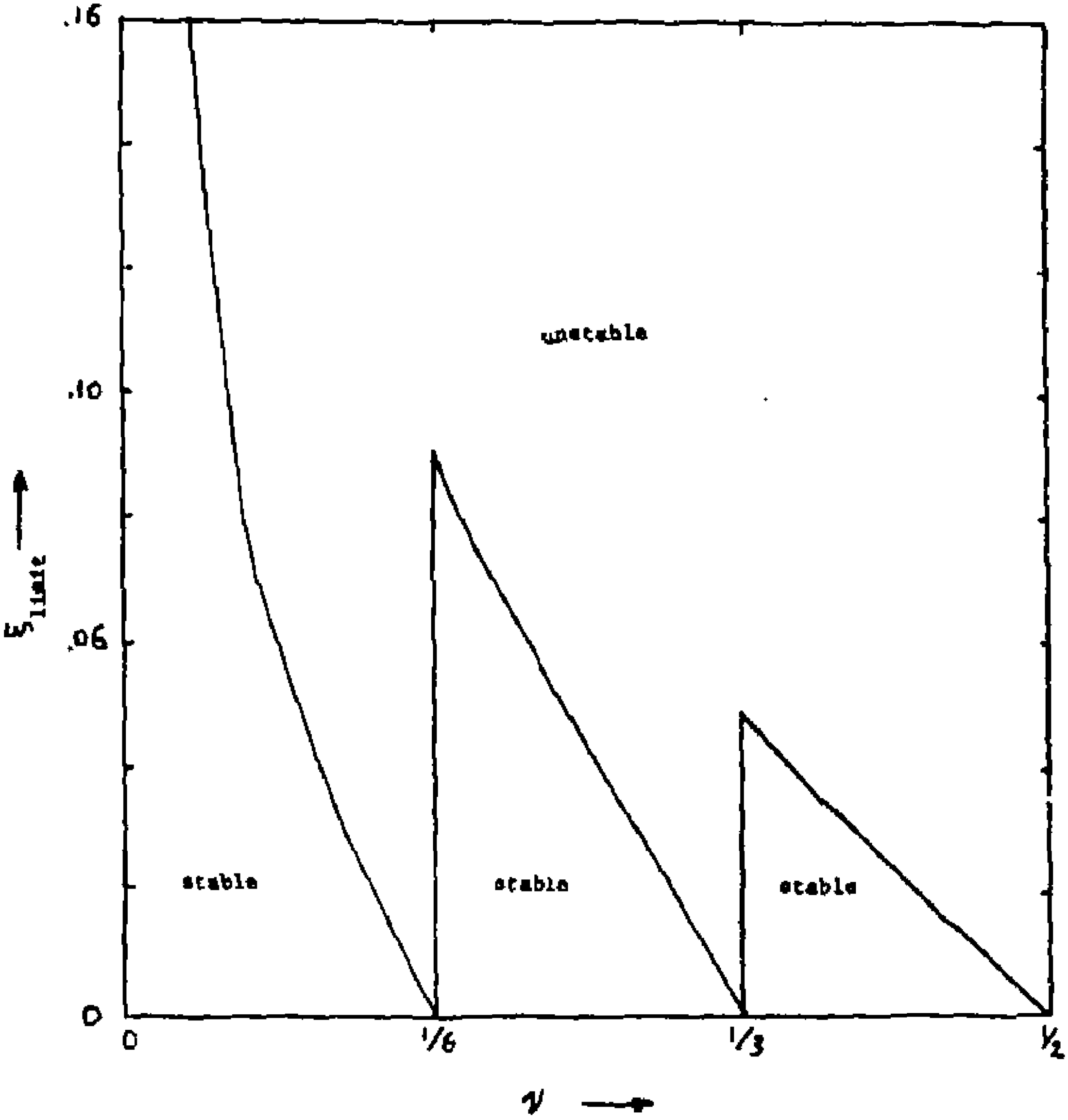

.16
.10
.06
0
ω_{limit}
unstable
stable
stable
stable
0
1/6
1/3
1/2
ν

F g. 8

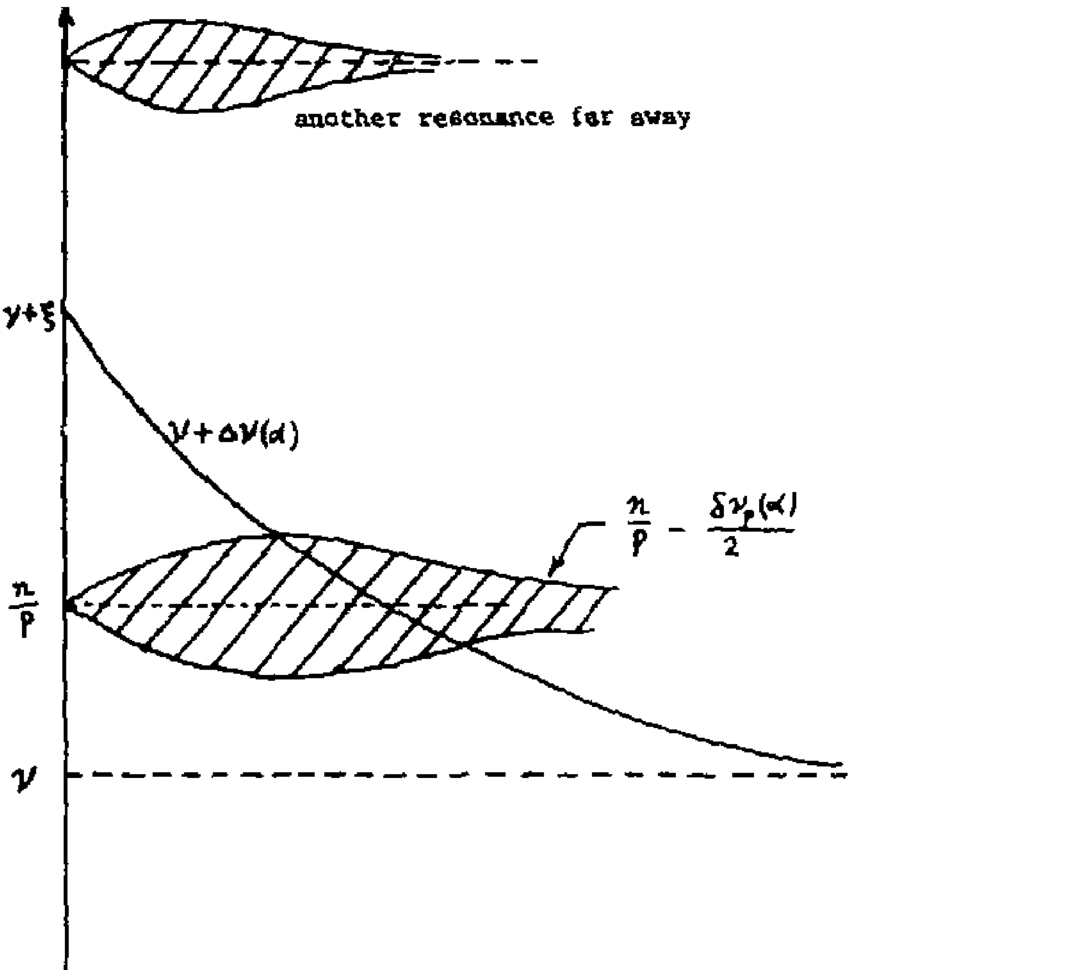

another resonance far away
$\nu+\xi$
$\nu+\Delta\nu(\alpha)$
$\frac{n}{p} - \frac{\delta\nu_p(\alpha)}{2}$
$\frac{n}{p}$
ν
α

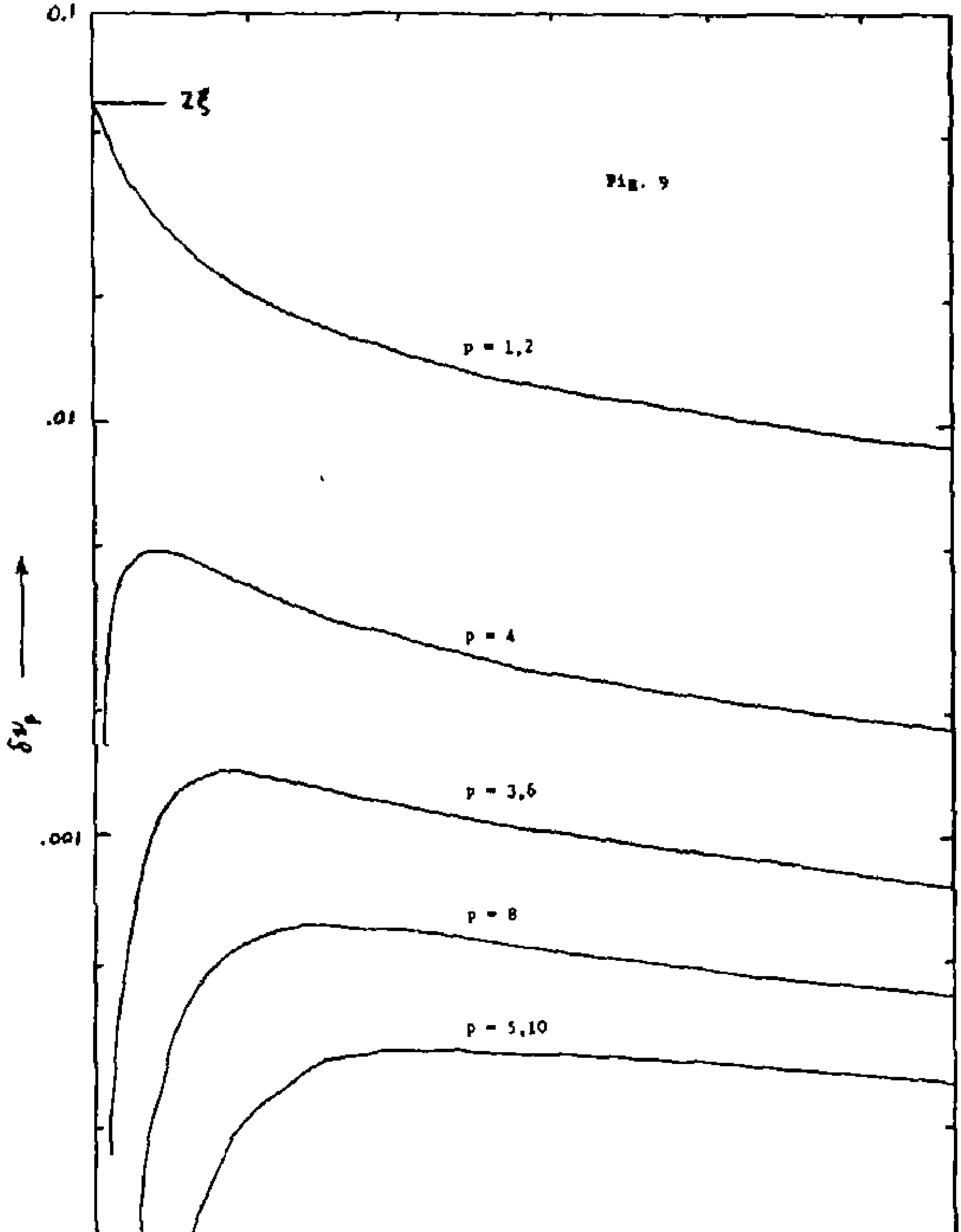

0.1
2ξ
Fig. 9
p = 1,2
.01
p = 4
p = 3,6
.001
p = 8
p = 5,10
.0001
20
40
α
δν_p

Fig. 10a

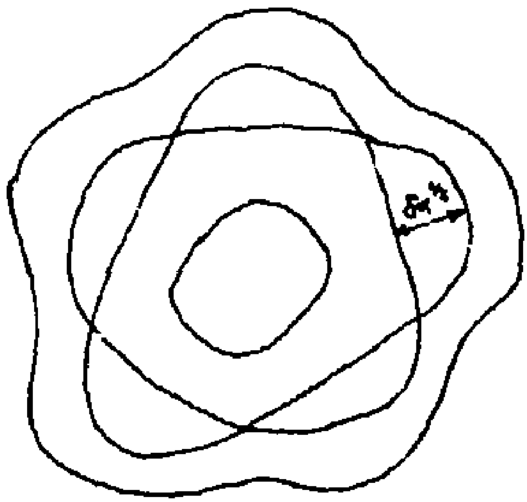

Fig. 10b

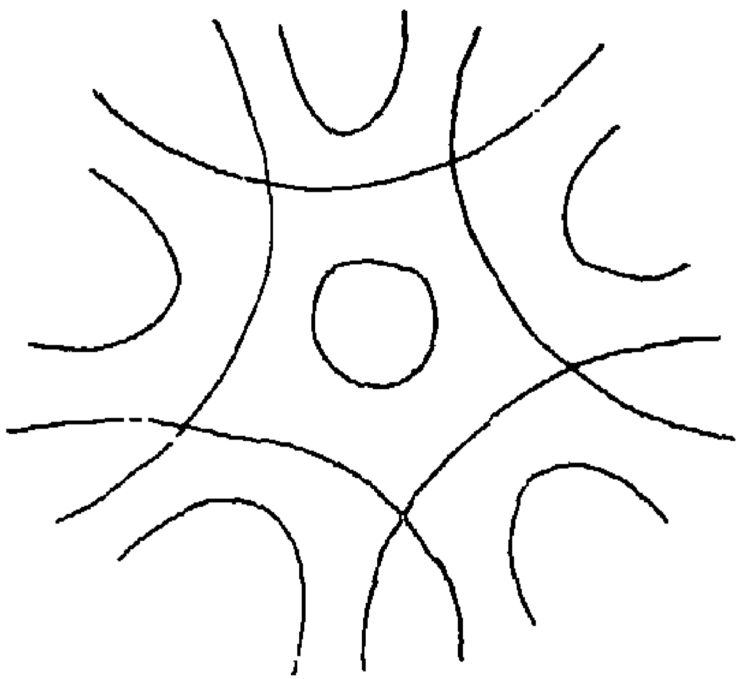

Fig. 11

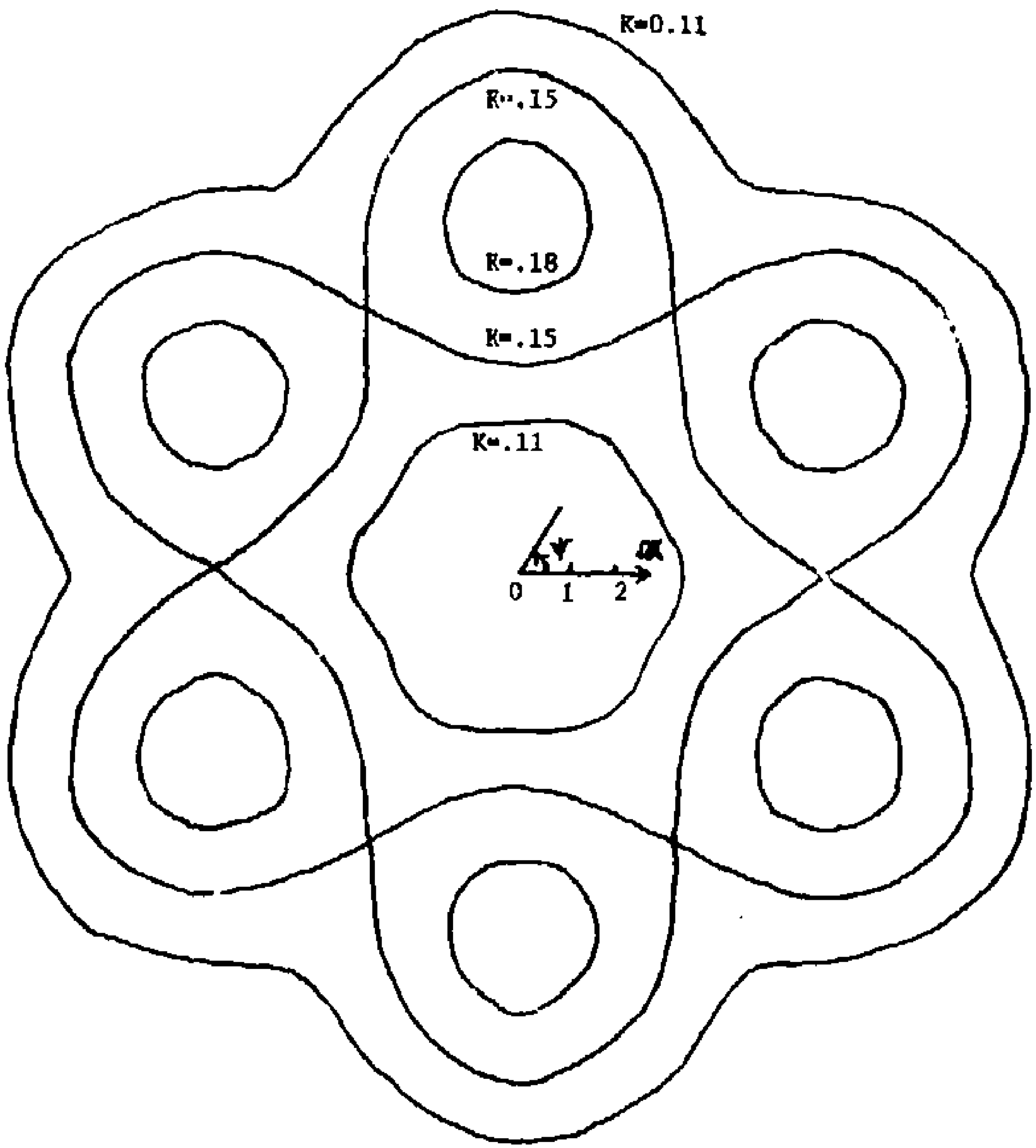

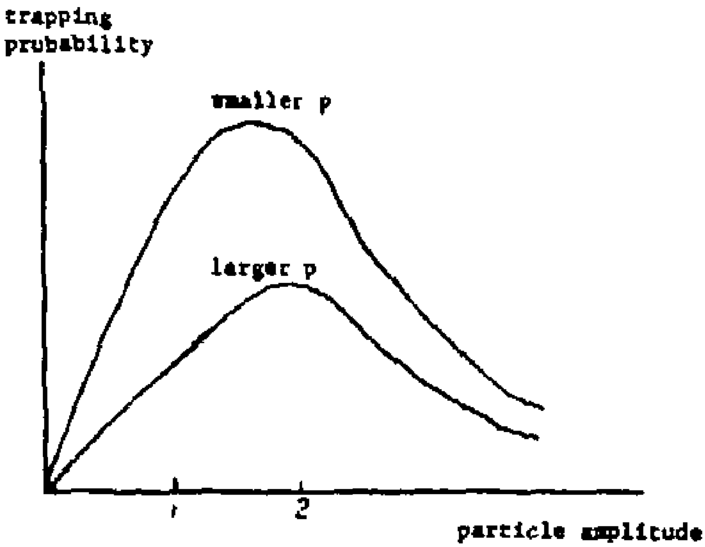

trapping
probability
smaller p
larger p
1
2
particle amplitude

Fig.12

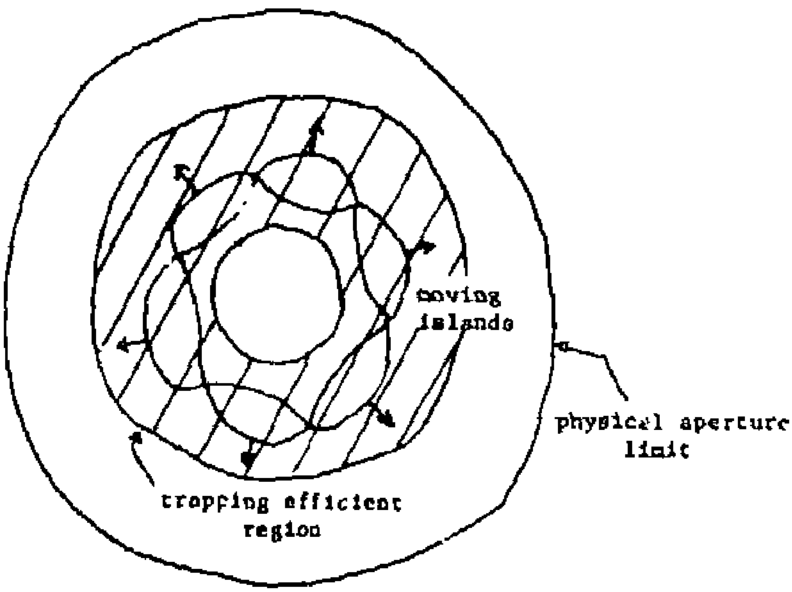

moving
islands
physical aperture
limit
trapping efficient
region

Fig. 13